Microscopic origins of quasi-static deformation in dense granular assemblies.

G. Combe & J.-N. Roux
Laboratoire Central des Ponts et Chaussées, Paris, France

ABSTRACT: We present numerical simulations of biaxial tests on dense packings of nearly rigid grains. Homogeneous samples are prepared under hydrostatic pressure, and then submitted to a stepwise increasing deviator stress. The use of both static and dynamical methods allows us to identify two different regimes according to whether macroscopic strains result from the mere deformations of the contacts themselves, or are essentially due to rearrangements of the packing. Some ensuing differences in terms of mechanical behaviour in the macroscopic limit of large systems are discussed.

1 INTRODUCTION

Discrete numerical simulation has become a basic tool for the study of microscopic origins of macroscopic mechanical behaviours of granular materials (Behringer & Jenkins 1997; Herrmann et al. 1998; Wolf & Grassberger 1997). Most often, one simply solves the differential equations stemming from Newton's law to compute the trajectories of collections of particles submitted to given external forces. Those numerical schemes, called *molecular dynamics* (DM) or 'distinct element methods', thus rely on a *dynamical* approach. Yet, dense granular assemblies submitted to slowly varying loads behave like solids, and the incremental stress-strain relations of traditional soil mechanics models are independent of physical time (Wood 1990). Theoretical approaches to micromechanics of grain packs also tend to focus on equilibrium situations. Moreover, they often deal with a fixed contact structure, whereas, under strain, the list of force-carrying contacts might change.

It is thus interesting to study in what sense the evolution of granular systems can be regarded as quasi-static, and in what situations macroscopic deformations imply rearrangements of the contact network. The work briefly reported here addresses both problems, in the simple case of the biaxial compression (Section 3) of the model granular systems presented in Section 2. Two different regimes of deformation are identified; possible consequences are discussed in the final part (Section 4).

2 MODEL. SAMPLE PREPARATION.

Collections of n disks, the diameters of which being uniformly distributed between 0.5 and 1 (the largest diameter is chosen as the unit length), are randomly generated and placed in a loose configuration within a square box in two dimensions. After some amount of mixing, using an energy-conserving algorithm to move the grains, with random initial velocities, as rigid impenetrable bodies in a fixed container, we proceed to an isotropic compaction of the sample. Two of the walls (marked 1 and 2 on fig. 1) are then free to move like pistons, constant principal stresses $\sigma_1 = F_1/L_2 = \sigma_2 = F_2/L_1 = p$ are imposed, with the notations of fig. 1 and the convention that tensile stresses are negative. In this compression step, disks are rigid

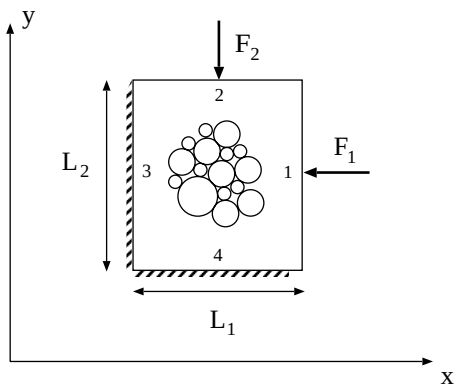

Figure 1: Schematic representation of isotropic and biaxial compressions of rectangular samples.

and devoid of friction, and an efficient energy dissi-

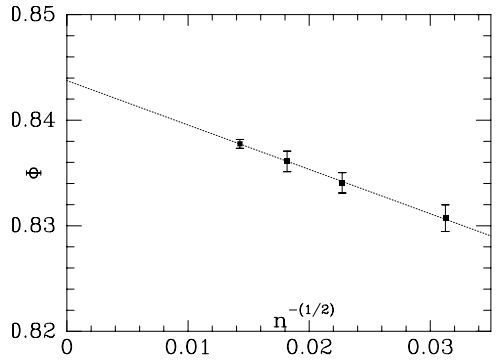

Figure 2: Packing fraction Φ versus $1/\sqrt{n}$, proportional to the ratio of perimeter to surface area in samples of n disks (51 for $n = 1024$, 23 for $n = 1936$ 10 for $n = 3025$, 18 for for $n = 4900$. Error bars extend to one standard deviation on each side of the average. The successful linear regression reflects the boundary effect and yields the estimated $n \to +\infty$ limit.

pation mechanism is introduced, until an equilibrium state is reached. We resort to the 'lubricated dynamics' method of refs. (Ouaguenouni & Roux 1997a; Ouaguenouni & Roux 1997b). This procedure assumes neighbouring grains to interact via a thin layer of a viscous lubricant, and produces final states in which both the equilibrium requirement (the net force on each grain is smaller than 10^{-4} for $p = 1$) and the impenetrability condition (interpenetration depth smaller than 10^{-7} in each contact) are accurately enforced. In particular, the force-carrying structure is then isostatic – a specific property of rigid frictionless disks or spheres (Roux 2000). Such compressions without friction produce dense homogeneous configurations. The packing fraction Φ associated with our preparation procedure is estimated in the large system limit (see Fig. 2) as 0.8437 ± 0.0012. Those configurations are the starting points of the biaxial tests that are studied in the sequel: denoting as L_i^0 the value of L_i (i =1 or 2) under the initial isotropic state of stress, one will stepwise increase stress deviator q by setting $\sigma_2 = F_2/L_1^0$ to $p + q$, while $\sigma_1 = F_1/L_2^0$ stays constant, equal to p. After each step Δq one waits for the next equilibrium state and then records strain parameters $\epsilon_i = -\Delta L_i/L_i^0$, or the relative area increase $\epsilon_v = -\epsilon_1 - \epsilon_2$. This is feasible as long as the 'deviator peak' is not reached: attempts to impose larger values of q, in such dense samples as ours, do not yet result in unbounded deformation and flow for the q domain investigated here. Most results given below do not pertain to perfectly rigid disks, but to packings in which the normal stiffness constant –assuming linear unilateral elasticity – is $K_N = 10^5 p$ in all contacts. Biaxial compression tests are studied here for disks with Coulomb friction in the contacts (the absence of friction in isotropic compaction is a device of the sample preparation procedure), the contact law is therefore elastoplastic in the following, with a tangential stiffness constant chosen as $K_T = K_N/2$. For the initial state to be in equilibrium with such characteristics and no mobilization of friction, one is led to a small final compression step, without friction (carried out by MD). Starting configurations are thus slightly denser (the increase in Φ can be estimated as $\Delta\Phi = (2.76 \pm 0.28) \times 10^{-5}$ as $n \to \infty$), while the degree of force indeterminacy (hyperstaticity) on the force-carrying structure (which comprises all but about 5.5% of the disks, the remaining ones being free to rattle in the 'cage' between their neighbours) stays smaller than $0.004n$.

3 BIAXIAL TESTS

3.1 *Strictly quasi-static regime.*

As intergranular friction is introduced, the degree of force indeterminacy at equilibrium (which vanishes for rigid, frictionless grains) takes a large, extensive (proportional to the number of degrees of freedom) value. The initially existing network of contacts might thus be expected to be able to sustain the load within some finite q interval. In order to be able to solve for the value of contact forces in this regime, one has, in view of this hyperstaticity, to introduce more material parameters than the sole friction coefficient μ. This is the essential reason why we had to deal with some elasticity in the contacts: even though the elastic part of the contact law might not be a physically accurate model, it enables, via an elastoplastic calculation, to obtain the complete system evolution (displacements, forces, status of the contacts) as long as the load is supported by the initial contact network. Such a computation, closely analogous to finite element methods applied to elastoplastic problems, only relies on static ingredients. We implemented the algorithm of ref. (Nguyen 1977), also used by (Bourada-Benyamina 1999) for discrete systems, within the approximation of small displacements, *i.e.*, neglecting geometrical changes (apart from opening of initially closed contacts). This latter approximation is well justified in the limit of rigid grains $K_N/p \to \infty$. As q increases, more and more contacts acquire a sliding status (with contact forces on the edge of the Coulomb cone), but the amplitude of the sliding is limited by the rest of the structure: plastic deformations are contained until macroscopic failure occurs. Displacements and strains, as functions of q, are thus, for a given network geometry, inversely proportional to K_N, and only depend, as well as forces, on μ and K_T/K_N. Meanwhile, a certain number of contacts open, especially among those that are oriented near the direction of extension. Consequently, the degree of force indeterminacy, assuming the status of contacts is known, *i.e.* counting, as in (Lanier & Jean 2000), only one unknown force value in sliding con-

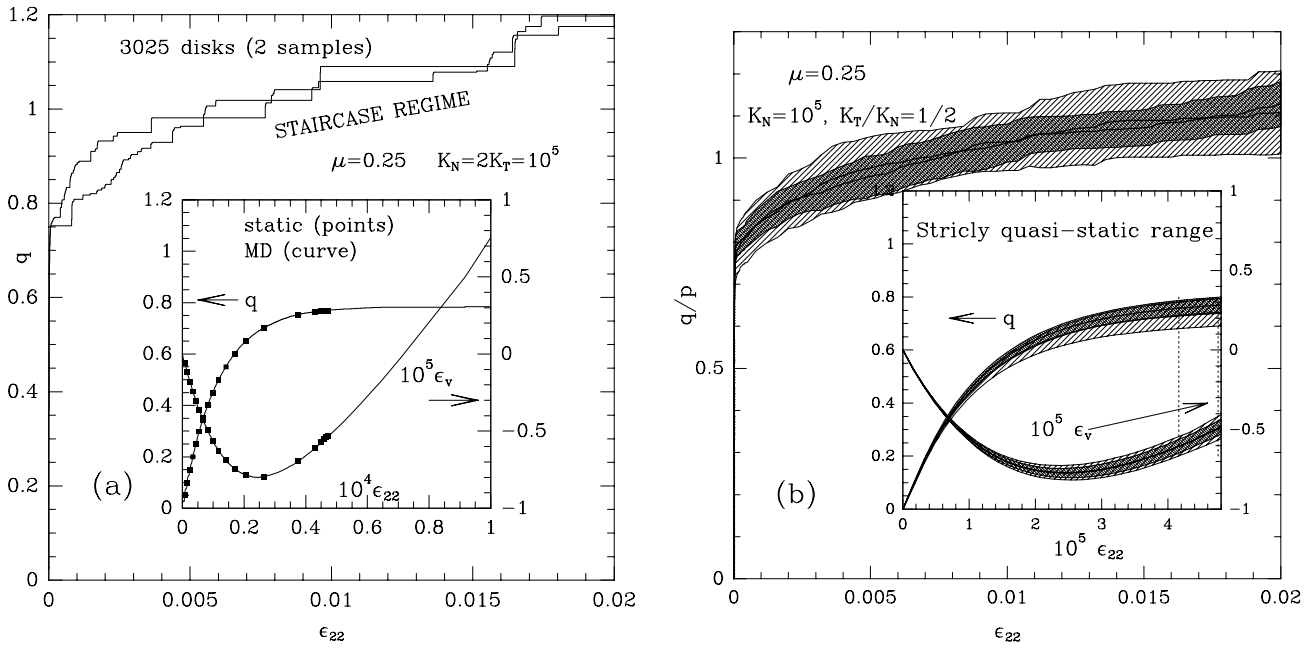

Figure 3: q and ϵ_v, as functions of ϵ_2. (a): q versus ϵ_2 in two $n = 3025$ samples : those curves exhibit the typical 'staircase' aspects of the rearrangement regime. The inset compares, for one sample, the results of the static (points) and the dynamic (continuous curves) methods, for $q < q_1$. Note the blown-up ϵ scale. (b): available DM results for $q(\epsilon_2)$ are averaged at constant ϵ_2, the shaded area extending one standard sample to sample deviation above and below the average. The darker region is for $n = 3025$, the lighter grey one for $n = 1024$. The inset presents the same data, along with ϵ_v, in the strictly quasi-static region: note the smaller fluctuations.

tacts, zero in open contacts, continuously decrases, from an initial value equal to the number n^* of force-carrying disks to less than $n^*/10$ at failure.

Calculations with different system sizes show very clearly that any value of q, however small, implies a non-vanishing density of sliding contacts in the large system limit: there is no purely elastic region in stress space. However, the largest supported deviator q_1 does possess a finite limit as $n \to \infty$, which, from calculations with 26 samples with $n = 1024$ and 26 samples with $n = 3025$, we estimate as $q_1 = 0.6 \pm 0.04$ for $\mu = 0.1$, $q_1 = 0.73 \pm 0.04$ for $\mu = 0.25$, and $q_1 = 1.10 \pm 0.08$ for $\mu = 0.5$. Interestingly, preliminary checks suggest that q_1, in each sample, is fairly insensitive to K_T/K_N.

Typical results for $\epsilon_2(q)$, $\epsilon_v(q)$ curves for $q < q_1$ are shown on Fig. 3. Such evolutions are quite smooth, as the response of the system to load increments is gradual and devoid of instability. Each point of the system trajectory in configuration space is an equilibrium state for a certain value of q: the evolution is indeed *quasi-static*.

Instead of those static computations, one can of course resort to more often employed dynamic procedures, such as MD, introducing the necessary additional parameters (inertia, viscous dissipation). This enables calculations beyond q_1, when the initial contact structure breaks apart. We carried out those simulations, with the same implementation of contact laws as in (Cundall & Strack 1979), increasing q by $\Delta q = 10^{-3}p$ steps, for 26 samples with $n = 1024$ and another 26 with $n = 3025$, with $\mu = 0.25$, keeping $K_N = 2K_T = 10^5 p$, until ϵ_2 reached the value 0.02. It is remarkable that the macroscopic response ($\epsilon_2(q)$, $\epsilon_v(q)$), sample by sample, is then undistinguishable from the static method result, as long as $q < q_1$ (see Fig. 3a). Moreover, provided the dynamic simulation is performed within the same small displacement approximation as the static one, both methods also appear to yield the same configuration at the microscopic level. This obviously calls for a theoretical study of uniqueness properties.

3.2 *Staircase regime.*

With all samples, q values significantly larger than q_1 are reached at $\epsilon_2 = 0.02$. Beyond q_1, new equilibrium states corresponding to higher q's have to involve new contacts which did not belong to the previous list. From the point of view of the initial contact network, failure implies the occurrence of unbounded deformation (a certain combination of sliding and opening of contacts that enables macroscopic motion). However, this incipient flow is soon arrested as newly formed contacts bring about new restrictions on the motion. This leads to a new equilibrium state. The amplitude of the motion from the former to the new configuration is now related to the distribution of open interstice thicknesses between neighbouring particles.

Its origin is geometric, it is no longer dictated by the contact law. As the system moves from one state to the next, it is not in equilibrium, and the specific chosen dynamics does matter. Its trajectory in configuration space is no longer quasi-static in the traditional sense, it consists in a (discrete) sequence of equilibria, separated by rearrangements. Hence the staircase aspect of the q-ϵ curve, Fig. 3a. Successive equilibria possess some interval of stability (corresponding to a nearly vertical part of the curve) with a fixed contact network, of a finite, yet small width: friction is still mobilized in a large number of contacts, and the degree of force indeterminacy remains small (as noted in (Lanier & Jean 2000)). The jerky aspect of strain variations and the large fluctuations in this *rearrangement* or *staircase regime* slows down the approach to any macroscopic limit. Whether the curve approaches a smooth limit is related to the distribution of stability intervals and of strain steps as a function of system size. Interestingly, a detailed statistical study allowed us to conclude that such a smooth curve – a macroscopic constitutive law for monotonous loading – does not exist for frictionless disks (Combe & Roux 2000). Here, the data collected with the two system sizes $n = 1024$ and $n = 3025$ (see Fig. 3b) indicate that a smooth limit can be expected, as the level of fluctuation about the average $q(\epsilon_2)$ gets smaller for the larger n. More detailed statistical investigations, involving another value of n, could be carried out. It would also be desirable to check for the influence of dynamical parameters on the statistics of the stress-strain evolution. If they can be shown to be irrelevant (as in the frictionless case (Combe & Roux 2000)) then the system trajectory could be termed 'quasi-static' in a broader sense, the relevant statistics being dictated by equilibrium properties alone.

4 DISCUSSION

Our essential result here is the existence of those two regimes, in which macroscopic strain is either due to deformations of the contacts, or to rearrangements, while the 'deviator peak' of the studied dense material is still not reached at a 2% 'axial' strain level. The possibility of doing calculations on a fixed contact network in a well defined range $q < q_1$ could be exploited in investigations of slow, gradual evolutions under cyclic loadings. From a fondamental point of view, two basic phenomena should be studied in detail at the microscopic level: the global failure of a network of elastoplastic contacts, and, once it occurred, the closing of intergranular interstices leading to possible new equilibrium configurations. These changes in the list of contacts gradually alter the distribution of contact orientations (Calvetti et al. 1997), presumably enabling new configurations to sustain larger deviators.

The transition, at growing deviator stress, from the strictly quasi-static to the staircase regime is reminiscent of the *characteristic state* of soil mechanics (Luong 1980; Tatsuoka & Ishihara 1974), at which the structure of the granular pack is supposed to be modified by large scale sliding motions and to 'disentangle'. It will be interesting to explore further whether some precise grain-level meaning can be attributed to this classical macroscopic concept.

REFERENCES

Behringer, R. P. & Jenkins, J. (Eds.) (1997). *Powders and Grains 97*, Rotterdam. Balkema.

Bourada-Benyamina, N. (1999). *Etude du comportement des milieux granulaires par homognisation priodique*. Ph. D. thesis, Ecole Nationale des Ponts et Chausses, Champs-sur-Marne, Frane.

Calvetti, F., Combe, G., & Lanier, J. (1997). Experimental micromechanical analysis of a 2d granular material: relation between structure evolution and loading path. *Mechanics of Cohesive-frictional materials 2*, 121–163.

Combe, G. & Roux, J.-N. (2000). Strain versus stress in a model granular material: a devil's staircase. *Phys. Rev. Lett. 85*, 3628–3631.

Cundall, P. A. & Strack, O. D. L. (1979). A discrete numerical model for granular assemblies. *Gotechnique 29*, 47–65.

Herrmann, H. J., Hovi, J.-P., & Luding, S. (Eds.) (1998). *Physics of Dry Granular Media*. Dordrecht: Balkema.

Lanier, J. & Jean, M. (2000). Experiment and simulations with 2d disk assemblies. *Powder Technology 109*, 206–221.

Luong, M.-P. (1980). Stress-strain aspects of cohesionless soils under cyclic and transient loading. In *Proc. Int. Symp. on Soil Under Cyclic and Transient Loading*, pp. 315–324. Balkema.

Ouaguenouni, S. & Roux, J.-N. (1997a). *Arching without Friction : a simple Model*, pp. 188–191. In Wolf & Grassberger (1997).

Ouaguenouni, S. & Roux, J.-N. (1997b). Force distribution in frictionless granular packings at rigidity threshold. *Europhys. Lett., 39*, 117–122.

Roux, J.-N. (2000). Geometric origin of mechanical properties of granular materials. *Phys. Rev. E 61*, 6802–6836.

Nguyen, Q. S. (1977). On the elastic-plastic initial boundary-value problem and its numerical integration. *Int. J. for Numerical Methods in Engineering 11*, 817–832.

Tatsuoka, F. & Ishihara, K. (1974). Drained deformatin of sand under cyclic stresses reversing direction. *Soils and Foundations 14*, 63–76.

Wolf, D. & Grassberger, P. (Eds.) (1997). *Friction, Arching, Contact Dynamics*. Singapore: World Scientific.

Wood, D. M. (1990). *Soil Behaviour and Critical State Soil Mechanics*. Cambridge University Press.